

UC Berkeley

UC Berkeley Previously Published Works

Title

Biospheric feedback effects in a synchronously coupled model of human and Earth systems

Permalink

<https://escholarship.org/uc/item/06g8g5wp>

Journal

Nature Climate Change, 7(7)

ISSN

1758-678X

Authors

Thornton, Peter E
Calvin, Katherine
Jones, Andrew D
[et al.](#)

Publication Date

2017-07-01

DOI

10.1038/nclimate3310

Peer reviewed

1 **Biospheric feedback effects in a synchronously coupled model of Earth and human systems**

2 Authors: Peter E. Thornton, Katherine Calvin, Andrew D. Jones, Alan V. Di Vittorio, Ben Bond-Lamberty, Louise
3 Chini, Xiaoying Shi, Jiafu Mao, William D. Collins, Jae Edmonds, Allison Thomson, John Truesdale, Anthony
4 Craig, Marcia L. Branstetter, George Hurtt [†]

5 **Fossil fuel combustion and land-use change are the first and second largest contributors to**
6 **industrial-era increases in atmospheric carbon dioxide concentration, which is itself the**
7 **largest driver of present-day climate change¹. Projections of fossil fuel consumption and**
8 **land-use change are thus fundamental inputs for coupled Earth system models (ESMs)**
9 **used to estimate the physical and biological consequences of future climate system**
10 **forcing^{2,3}. While historical datasets are available to inform past and current climate**
11 **analyses^{4,5}, assessments of future climate change have relied on projections of energy and**
12 **land use from energy economic models, constrained by assumptions about future policy,**
13 **land-use patterns, and socio-economic development trajectories⁶. Here we show that the**
14 **influence of biospheric change (i.e., the integrated effect of climatic, ecological, and**
15 **biogeochemical processes) on land ecosystems drives significant feedbacks in energy,**
16 **agriculture, land-use, and carbon cycle projections for the 21st century. Previous ESM**

[†] Present addresses: P.E.T., X.S., and J.M., Oak Ridge National Laboratory, Environmental Sciences Division/Climate Change Science Institute; K.C., B.B.-L., and J.E., Joint Global Change Research Institute, Pacific Northwest National Laboratory; A.D.J., A.V.D., and W.D.C., Lawrence Berkeley National Laboratory; L.C. and G.H., University of Maryland; J.T. and A.C., independent contractors with Lawrence Berkeley National Laboratory; M.L.B., Oak Ridge National Laboratory, Computer Science and Mathematics Division/Climate Change Science Institute; A.T., Field to Market: The Alliance for Sustainable Agriculture, 777 N Capitol St NE, Washington, DC 20002.

Copyright Notice: This manuscript has been authored by UT-Battelle, LLC under Contract No. DE-AC05-00OR22725 with the U.S. Department of Energy. The United States Government retains and the publisher, by accepting the article for publication, acknowledges that the United States Government retains a non-exclusive, paid-up, irrevocable, world-wide license to publish or reproduce the published form of this manuscript, or allow others to do so, for United States Government purposes. The Department of Energy will provide public access to these results of federally sponsored research in accordance with the DOE Public Access Plan(<http://energy.gov/downloads/doe-public-access-plan>).

17 **studies of future climate have ignored these biospheric feedbacks with human systems. We**
18 **find that exposure of land ecosystem productivity in the economic system to biospheric**
19 **change as it develops in an ESM results in a 10% reduction of land area used for crop**
20 **cultivation; increased managed forest area and land carbon; a 15-20% decrease in global**
21 **crop price; and a 17% reduction in fossil fuel emissions for a low-mid range forcing**
22 **scenario⁷. These results demonstrate that biospheric change can significantly alter primary**
23 **human system forcings to the climate system, and that these interactions are handled**
24 **inconsistently, or excluded altogether, in the one-way asynchronous coupling of energy**
25 **economic models to ESMs to date^{1, 8-9}.**

26 Current projections of future climate are based on ESMs that include sophisticated
27 representations of biotic and abiotic processes in the Earth system, but which represent human
28 systems through static, unidirectional, asynchronous coupling¹⁰ (black arrows in Figure 1a). We
29 explore here the difference between asynchronous coupling, in which human system models are
30 executed in advance to generate complete time series outputs later passed to an ESM, and
31 synchronous coupling, in which the human system model and ESM are executed simultaneously,
32 with opportunity for interaction between these two components that can change the simulation
33 trajectory of both. In the traditional asynchronous approach, human system information required
34 as forcing for climate prediction is generated in advance by economic integrated assessment
35 models (IAMs) that include both energy and agricultural sectors. As summarized in the Fifth
36 Assessment Report of the Intergovernmental Panel on Climate Change (AR5), several IAMs
37 have been used to generate standard climate forcing inputs to ESMs covering a range of policy
38 assumptions from aggressive mitigation to business-as-usual^{1,11}. These inputs include
39 harmonized forcings sharing a common historical baseline and a common set of definitions and

40 analyses for 21st century long-lived¹² and short-lived¹³ greenhouse gas (GHG) emissions and
41 land-use change⁵.

42 IAM projections of future GHG and air pollutant emissions and land-use and land-cover change
43 (LULCC) are constrained by assumptions regarding human demography, economic development
44 trajectories, and policy. Estimates of ecosystem productivity and crop yields (including biomass
45 energy crops for some scenarios) are based on historical data. These estimates change over time,
46 following assumptions about the influence of technological change on yield and endogenous
47 estimates of crop location and area (Figure 1a). IAMs do not typically consider the influence of
48 future biospheric change, although recent work has evaluated the economic and carbon stock
49 impacts of changing temperature, precipitation, and atmospheric carbon dioxide concentration
50 ($CO_{2,atm}$) in crop and land-use models^{14,15}.

51 The use of asynchronous coupling in climate projections for AR5 excludes the influence of
52 multiple biospheric factors known to influence managed ecosystems, including short-term
53 weather variation¹⁶, long-term climate trends¹⁷, changes in $CO_{2,atm}$ ^{18,19}, changes in atmospheric
54 deposition of reactive nitrogen on land²⁰, and the complex interactions among these factors^{21,22}.

55 One IAM used in AR5, the IMAGE model, does have the capability to examine the dynamic
56 influence of climate change factors on ecosystem productivity using its own internal, reduced-
57 form climate model²³, but its scenarios for use by ESMs are still based on one-way coupling and
58 result in inconsistent representation of biospheric change between the IAM and ESM. Two-way
59 coupling of IMAGE to a general circulation model (GCM) was used to examine changes in land
60 use²⁴, but the feedback in that case was limited by passing only 30-year mean monthly
61 temperature and precipitation changes from the GCM to IMAGE. In that study, simulation of
62 carbon cycle and ecosystem processes was performed within IMAGE, a simple and highly

63 parameterized land model which ignores the tight integration of biophysical and biogeochemical
64 processes, driven by sub-daily variations in temperature, precipitation, humidity, and short and
65 long-wave radiation. This mechanistic coupling of biological and physical processes at the land
66 surface-atmosphere interface is a defining feature of the current generation of ESMs¹.

67 Here we investigate the influence of biospheric change on human systems and associated
68 feedbacks to the biosphere as introduced in a synchronous two-way coupling approach. We
69 introduce two-way coupling by passing biospheric change information from an ESM to the
70 ecosystem productivity and crop yield components of an IAM at five-year intervals, as
71 radiatively-forced climate change unfolds over the course of a 90-year simulation (2005-2094).
72 We examine the consequences of realistic two-way feedback between the human and Earth
73 system components for crop price, fossil fuel emissions, LULCC, and transfers of carbon
74 between land, ocean, and atmosphere (Figure 1b). The IAM component used here is the Global
75 Change Assessment Model (GCAM 3.0)²⁵ and the ESM is the Community Earth System Model
76 (CESM 1.1)²⁶. We refer to the two-way coupled system as the integrated Earth system model
77 (iESM)²⁷. Our investigation uses the same demographic and policy assumptions as the 4.5 W m⁻²
78 radiative forcing reference concentration pathway (RCP4.5) scenario of AR5⁷, which was
79 originally generated by GCAM. The passing of LULCC signals from IAM to ESM is based on
80 the land-use harmonization approach used in AR5⁵, with modifications to improve signal
81 integrity⁸. To help assess the generality of our results, we also performed a pair of simulation
82 experiments based on a the AR5 RCP 8.5 scenario

83 [insert Figure 1 here]

84 Coupling from ESM to IAM is accomplished by passing an integrated biospheric change signal
85 to each of the IAM spatial units and land types at five-year intervals. This signal is based on
86 departures from a present-day baseline (average over period 2000-2004) of net primary
87 production and heterotrophic respiration generated by the ESM land model component, which
88 includes a fully prognostic treatment of energy, water, carbon, and nitrogen cycles for multiple
89 vegetation types in each ESM land grid cell. This signal captures the desired change factors with
90 minimal bias and a linear response, while minimizing signal interference from LULCC²⁸.

91 The global average of the productivity and yield component of this signal is similar in magnitude
92 and time course among the major vegetated land types, increasing by about 10% by 2094 (Figure
93 2), with regional variation reflecting patterns of changed ecosystem productivity in the ESM
94 (Supplemental Figure 2). In CESM, land productivity tends to increase under climate change
95 scenarios, driven primarily by increasing atmospheric CO₂ concentration and anthropogenic
96 nitrogen deposition associated with fossil fuel combustion, overlain with spatially and temporally
97 varying effects due to increasing temperature and changing precipitation patterns. Even though
98 CESM, with its inclusion of carbon-nitrogen cycle coupling, generates one of the lowest CO₂
99 fertilization effects in the CMIP5 collection of ESMs, the CO₂ fertilization effect still dominates
100 the varying climate feedbacks to produce global-scale patterns of increasing land productivity
101 under all tested scenarios¹. Nothing we have added to the iESM system alters these ESM-centric
102 aspects of the ecosystem-climate feedbacks, and the increasing productivity obtained in our
103 iESM experiments is qualitatively and quantitatively consistent with the well-characterized
104 behavior of CESM in this regard. The unique aspect of our study is that this increased
105 productivity is communicated synchronously to the human system component to influence
106 LULCC (and other energy economic factors such as crop price and fossil fuel emissions). Our

107 estimate of 10% increase in ecosystem productivity and crop yield over present-day is consistent
108 with estimates from free-air CO₂ enrichment (FACE) studies for crop yield¹⁸. CO_{2,atm} prognosed
109 in the ESM rises to approximately 590 parts per million by volume by 2094 in the two-way
110 coupled simulation (Supplemental Figure 3), similar to the enriched levels typical of FACE
111 experiments, although a direct comparison of model and experimental results in this case suffers
112 from differences in the time scale of changed forcing and the integration in our simulations of
113 additional factors such as changing climate and changing rates of nutrient inputs and
114 mineralization. Our finding of increased productivity under future climate change contrasts with
115 recent results reported for a comparison of agricultural models, but that study excluded the
116 possibility of CO₂ fertilization¹⁴. Other recent work has stressed the importance of modeled
117 nutrient dynamics in estimating CO₂ fertilization for global cropland²², a factor included in our
118 ESM.

119 [insert Figure 2 here]

120 We quantify the influence of coupling approaches by differencing two simulations, one with
121 two-way synchronous coupling and the other with traditional one-way asynchronous coupling. A
122 common trajectory for fossil fuel emissions is used in both simulations (discussed below). Global
123 crop prices increase through 2080 for both coupling approaches under RCP4.5, driven by a
124 mitigation policy that applies a cost to carbon emissions²⁵ (Supplemental Figure 4), but the
125 increase in price is 12-25% smaller in the synchronously coupled system (Figure 3a), with
126 similar magnitude and trajectory for major crop types. The decline in prices under the
127 experimental simulation is due to higher productivity (Supplemental Figure 5) that reduces
128 cropland requirements and lessens competition for land. Higher productivity with biospheric
129 feedback drives a 10% decrease in total global crop area, as the same amount of food and feed

130 can be produced on smaller amounts of land. The decrease in total global crop area is
131 accompanied by an increase in area of noncommercial forest (Figure 3b).

132 [insert Figure 3 here]

133 These changes drive carbon cycle responses in the land model component of the ESM, resulting
134 in altered $\text{CO}_{2,\text{atm}}$. Atmospheric change drives additional response in the ocean carbon cycle
135 through physical and biological feedbacks with $\text{CO}_{2,\text{atm}}$ (Figure 1b, pathways labeled 3, 4, and
136 5). Specifically, land ecosystems accumulate 5-10 Pg of additional carbon with two-way
137 coupling, driving a decrease in $\text{CO}_{2,\text{atm}}$ that in turn reduces the amount of carbon transferred from
138 the atmosphere to the ocean by ~ 3 Pg C (Figure 4). Variability in this feedback flux on
139 interannual to decadal timescales is suggested by the two ensemble members, superimposed on a
140 coupling signal with peak increase in land carbon storage around 2060. This peak and
141 subsequent decline corresponds in time with a reduced rate of increase in non-commercial forest
142 area (Figure 3b).

143 [insert Figure 4 here]

144 Increases in ecosystem productivity and crop yield, combined with decreases in the global land
145 area required for food, feed, and fiber crops drive increases in bioenergy potential and
146 corresponding decreases in the price of bioenergy. The decline in bioenergy cost results in an
147 increase in demand, an increase in land area dedicated to biomass energy production (Figure 3b),
148 and a decline in the demand of other energy carriers (e.g., gas and coal). The decrease in carbon-
149 intensive energy production leads to a 17% reduction in predicted fossil fuel emissions by the
150 end of the 21st century (Supplemental Figure 6). The changes in global carbon stocks shown in
151 Figure 4 do not reflect the lower fossil fuel emissions generated by the biospheric feedback, as

152 we held these emissions constant for the two simulations to provide the least complicated
153 feedback demonstration. We expect that a more complete coupling, in which the updated fossil
154 fuel emissions are passed to the ESM, would result in lower atmospheric concentrations, less
155 land carbon storage via CO₂ fertilization in the ESM land model, and a decreased rate of ocean
156 carbon uptake.

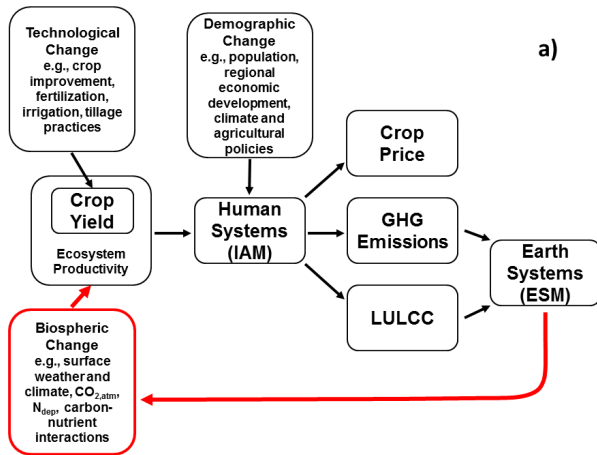
157 We obtain qualitatively similar results when comparing asynchronous one-way coupling and
158 synchronous two-way coupling under a higher radiative forcing scenario (RCP 8.5). Biospheric
159 change caused increases in crop yield of 15-22% for RCP 8.5, compared to 11-17% increase for
160 RCP 4.5 (Supplemental Figure 8). Two-way coupling causes a decrease in crop prices of 6-17%
161 for RCP 8.5, compared to 12-25% decrease for RCP 4.5. Changes in yield and price drive shifts
162 in LULCC that are somewhat larger for RCP 8.5 than for RCP 4.5, while acting through similar
163 mechanisms. The land ecosystem accumulates an additional 10-15 PgC due to two-way coupling
164 by the final decades of RCP 8.5, compared to 5-10 PgC additional accumulation for RCP 4.5.

165 We conclude that biospheric feedbacks to human systems can significantly alter primary
166 anthropogenic climate forcing by driving changes in land use and energy activities which
167 propagate to changes in land, atmosphere, and ocean carbon stocks as well as changes in fossil
168 fuel emissions trajectories: truly comprehensive climate change assessment efforts must
169 therefore consider these feedbacks. The approach demonstrated here removes a major
170 inconsistency in the practice of coupled Earth system modeling as identified in AR5¹, thereby
171 improving the policy relevance of climate and Earth system model projections^{29,30}. Our study
172 does not seek to provide a comprehensive assessment of uncertainty associated with a particular
173 scenario. Indeed, a synchronously coupled system that includes an ESM component can never
174 replace the traditional use of stand-alone IAMs as tools for deep exploration of uncertainty.

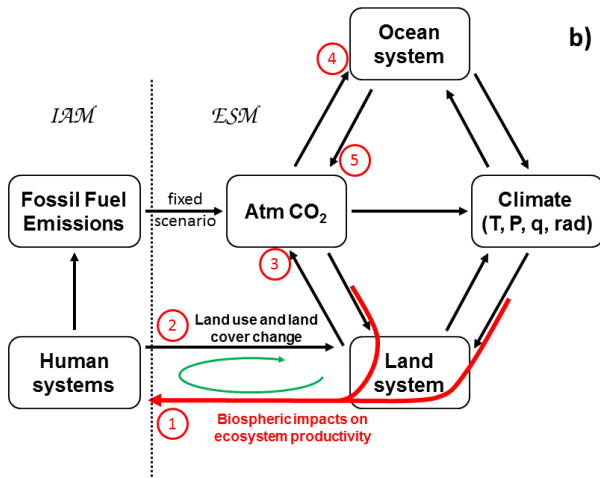
Thornton, Peter E. 8/21/2016 12:40 PM

Comment [1]: These numbers still to be updated when the final years of analysis are available from Kate.

175 Instead, we argue that the synchronously coupled system is a new tool that allows us to explore a
176 previously dark region of the uncertainty space: each time an ESM is run without synchronous
177 coupling we miss an opportunity to better understand and quantify this uncertainty.



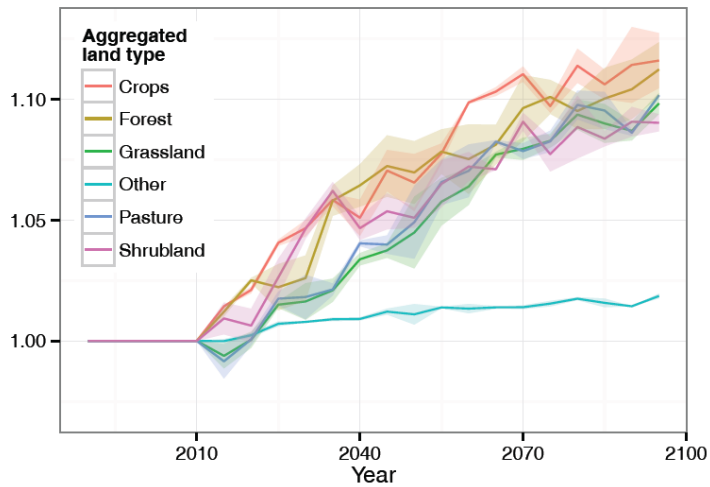
179



180

181 **Figure 1. Interactions between human and Earth systems using one-way (black) and two-**
 182 **way (black + red) coupling. a) Technological change factors for crop yield are included in the**
 183 **generation of IAMs used for AR5, but biospheric change factors are not. Demographic**

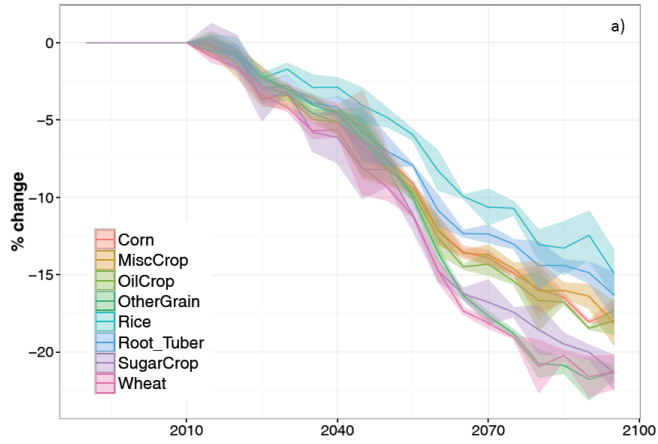
184 constraints and policy assumptions are necessary IAM inputs, with important influence on
185 projected crop price, GHG emissions, and LULCC. Ecosystem productivity, including crop
186 yield, has been considered as a static input to IAMs in AR5. Red arrows indicate the new
187 feedback connections in our study, passing biospheric change information from the ESM back to
188 the IAM through its influence on ecosystem productivity and crop yield. **b)** For AR5,
189 connections across the dotted line are asynchronous and one-way (from IAM to ESM).
190 Synchronous two-way coupling described here is accomplished by passing biospheric
191 information, as filtered by the ESM land model component, to the IAM on a 5-year time step
192 (red arrows, pathway labeled 1). This new information drives LULCC changes that are passed
193 back to the land system (pathway labeled 2), resulting in a coupled feedback (green arrow). T, P,
194 q, rad indicate temperature, precipitation, humidity, and radiation components of physical
195 climate.



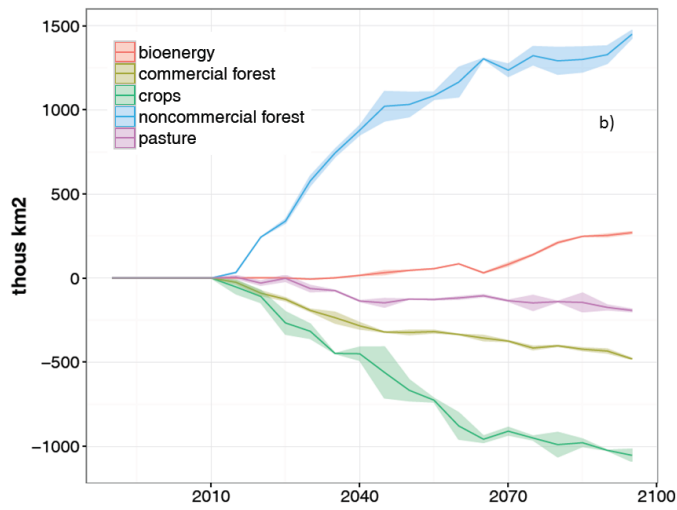
197

198 **Figure 2. Integrated biospheric change for the 21st century, as communicated from ESM to**
 199 **IAM.** The scalar used to inform ecosystem productivity and crop yield changes in the IAM
 200 includes a vegetation component (shown here) based on change in net primary production
 201 relative to conditions in 1990 and a below ground component based on changes in net primary
 202 production and heterotrophic respiration (Supplemental Figure 1). Category “Other” includes
 203 urban, lake, land ice, and bare ground. The signal communicated to the IAM is specific to each
 204 agro-ecological zone and vegetation type within zone, with the plot showing area-weighted
 205 global mean signal. For each aggregated land type the solid colored line shows the mean of two
 206 ensemble simulations, while the shaded region of matching color shows the range of values from
 207 the two ensemble members.

208



209



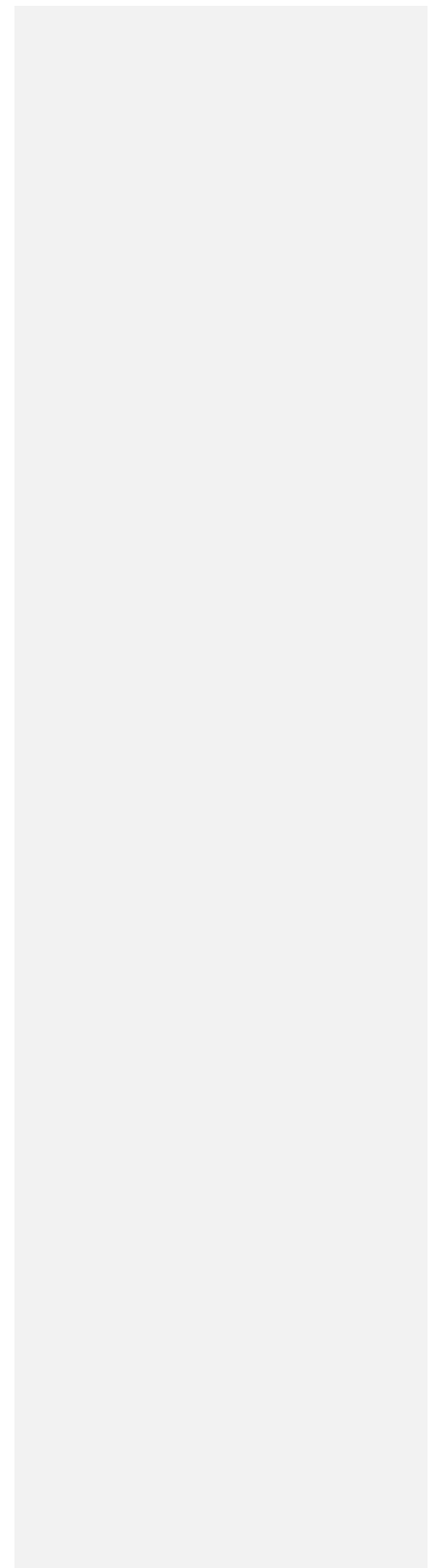
210

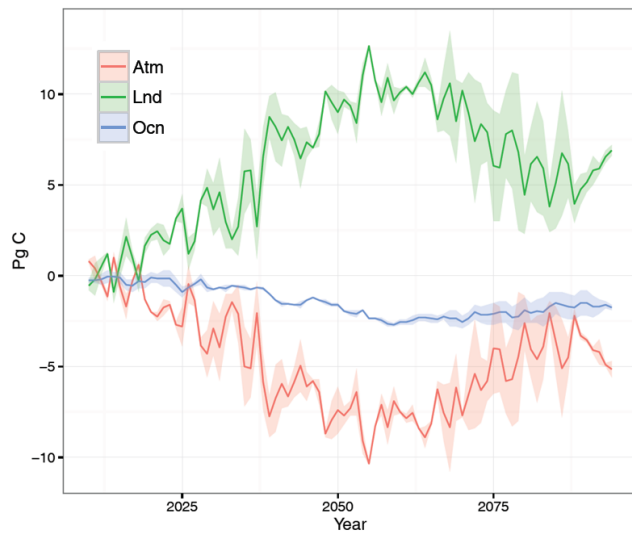
211 **Figure 3. Changes in crop price and land-use area resulting from biospheric feedback. a)**

212 Percentage change in global average crop price, relative to the asynchronous one-way coupling

213 (control) simulation, for each major crop type. b) Global total change in land cover summarized
214 by major land-use/land-cover types, relative to the asynchronous one-way coupling simulation.
215 For each aggregated crop type or land cover type the solid colored line shows the mean of two
216 ensemble simulations, while the shaded region of matching color shows the range of values from
217 the two ensemble members.

218





219

220 **Figure 4. Change in global carbon stocks caused by biospheric feedback to human systems.**

221 Difference in total carbon stocks on land, in the atmosphere, and in the oceans, between two-way
 222 and one-way coupling simulations, as predicted within the ESM component of our coupled
 223 system. Solid colored line shows the mean of two ensemble members, while the shaded region
 224 of matching color shows range of values from the two ensemble members.

225

226

- 228 1 IPCC. *Climate Change 2013: The Physical Science Basis. Contribution of Working Group I to the*
229 *Fifth Assessment Report of the Intergovernmental Panel on Climate Change* (eds T.F. Stocker *et*
230 *al.*) 1535 pp (Cambridge University Press, Cambridge, United Kingdom and New York, NY, USA,
231 2013).
- 232 2 Hoffman, F. M. *et al.* Causes and implications of persistent atmospheric carbon dioxide biases in
233 Earth System Models. *Journal of Geophysical Research: Biogeosciences* **119**, 141-162,
234 doi:10.1002/2013JG002381 (2014).
- 235 3 Shevliakova, E. *et al.* Carbon cycling under 300 years of land use change: Importance of the
236 secondary vegetation sink. *Global Biogeochemical Cycles* **23**, 1-16,
237 doi:doi:10.1029/2007GB003176 (2009).
- 238 4 Andres, R. J. *et al.* A synthesis of carbon dioxide emissions from fossil-fuel combustion.
239 *Biogeosciences* **9**, 1845-1871, doi:10.5194/bg-9-1845-2012 (2012).
- 240 5 Hurtt, G. *et al.* Harmonization of land-use scenarios for the period 1500–2100: 600 years of
241 global gridded annual land-use transitions, wood harvest, and resulting secondary lands.
242 *Climatic Change* **109**, 117-161, doi:10.1007/s10584-011-0153-2 (2011).
- 243 6 Moss, R. H. *et al.* The next generation of scenarios for climate change research and assessment.
244 *Nature* **463**, 747-756,
245 doi:http://www.nature.com/nature/journal/v463/n7282/supinfo/nature08823_S1.html
246 (2010).
- 247 7 Thomson, A. *et al.* RCP4.5: a pathway for stabilization of radiative forcing by 2100. *Climatic*
248 *Change* **109**, 77-94, doi:10.1007/s10584-011-0151-4 (2011).
- 249 8 Di Vittorio, A. V. *et al.* From land use to land cover: restoring the afforestation signal in a
250 coupled integrated assessment–earth system model and the implications for CMIP5 RCP
251 simulations. *Biogeosciences* **11**, 6435-6450, doi:10.5194/bg-11-6435-2014 (2014).
- 252 9 Jones, A. D. *et al.* Greenhouse Gas Policy Influences Climate via Direct Effects of Land-Use
253 Change. *Journal of Climate* **26**, 3657-3670, doi:10.1175/JCLI-D-12-00377.1 (2013).
- 254 10 Ciais, P. *et al.* in *Climate Change 2013: The Physical Science Basis. Contribution of Working Group*
255 *I to the Fifth Assessment Report of the Intergovernmental Panel on Climate Change* (eds T.F.
256 Stocker *et al.*) (Cambridge University Press, Cambridge, United Kingdom and New York, NY, USA,
257 2013).
- 258 11 van Vuuren, D. *et al.* The representative concentration pathways: an overview. *Climatic Change*
259 **109**, 5-31, doi:10.1007/s10584-011-0148-z (2011).
- 260 12 Meinshausen, M. *et al.* The RCP greenhouse gas concentrations and their extensions from 1765
261 to 2300. *Climatic Change* **109**, 213-241, doi:10.1007/s10584-011-0156-z (2011).
- 262 13 Lamarque, J.-F. *et al.* Global and regional evolution of short-lived radiatively-active gases and
263 aerosols in the Representative Concentration Pathways. *Climatic Change* **109**, 191-212,
264 doi:10.1007/s10584-011-0155-0 (2011).
- 265 14 Nelson, G. C. *et al.* Climate change effects on agriculture: Economic responses to biophysical
266 shocks. *Proc. Natl. Acad. Sci. U. S. A.* **111**, 3274-3279, doi:10.1073/pnas.1222465110 (2014).
- 267 15 Humpenöder, F. *et al.* Land-Use and Carbon Cycle Responses to Moderate Climate Change:
268 Implications for Land-Based Mitigation? *Environmental Science & Technology* **49**, 6731-6739,
269 doi:10.1021/es506201r (2015).
- 270

- 271 16 Ruane, A. C. *et al.* Climate change impact uncertainties for maize in Panama: Farm information,
272 climate projections, and yield sensitivities. *Agricultural and Forest Meteorology* **170**, 132-145,
273 doi:<http://dx.doi.org/10.1016/j.agrformet.2011.10.015> (2013).
- 274 17 Welch, J. R. *et al.* Rice yields in tropical/subtropical Asia exhibit large but opposing sensitivities
275 to minimum and maximum temperatures. *Proceedings of the National Academy of Sciences* **107**,
276 14562-14567, doi:10.1073/pnas.1001222107 (2010).
- 277 18 Long, S. P., Ainsworth, E. A., Leakey, A. D. B., Nösberger, J. & Ort, D. R. Food for thought: lower-
278 than-expected crop yield stimulation with rising CO₂ concentrations. *Science* **312**, 1918-1921,
279 doi:doi: 10.1126/science.1114722 (2006).
- 280 19 Norby, R. J. *et al.* Forest response to elevated CO₂ is conserved across a broad range of
281 productivity. *Proceedings of the National Academy of Sciences* **102**, 18052-18056 (2005).
- 282 20 Sutton, M. A. *et al.* Uncertainties in the relationship between atmospheric nitrogen deposition
283 and forest carbon sequestration. *Global Change Biology* **14**, 2057-2063, doi:10.1111/j.1365-
284 2486.2008.01636.x (2008).
- 285 21 Norby, R. J., Warren, J. M., Iversen, C. M., Medlyn, B. E. & McMurtrie, R. E. CO₂ enhancement of
286 forest productivity constrained by limited nitrogen availability. *Proc. Natl. Acad. Sci. U. S. A.* **107**,
287 19368-19373, doi:10.1073/pnas.1006463107 (2010).
- 288 22 Rosenzweig, C. *et al.* Assessing agricultural risks of climate change in the 21st century in a global
289 gridded crop model intercomparison. *Proceedings of the National Academy of Sciences* **111**,
290 3268-3273, doi:10.1073/pnas.1222463110 (2014).
- 291 23 Stehfest, E. *et al.* *Integrated Assessment of Global Environmental Change with IMAGE 3.0. Model*
292 *description and policy applications.*, 370 pp (The Hague: PBL Netherlands Environmental
293 Assessment Agency, 2014).
- 294 24 Voldoire, A., Eickhout, B., Schaeffer, M., Royer, J.-F. & Chauvin, F. Climate simulation of the
295 twenty-first century with interactive land-use changes. *Climate Dynamics* **29**, 177-193,
296 doi:10.1007/s00382-007-0228-y (2007).
- 297 25 Wise, M., Calvin, K., Kyle, P., Luckow, P. & Edmonds, J. Economic and physical modeling of land
298 use in GCAM 3.0 and an application to agricultural productivity, land, and terrestrial carbon. .
299 *Climate Change Economics* **05**, 1450003, doi:doi:10.1142/S2010007814500031 (2014).
- 300 26 Hurrell, J. W. *et al.* The Community Earth System Model: A Framework for Collaborative
301 Research. *Bulletin of the American Meteorological Society* **94**, 1339-1360, doi:10.1175/BAMS-D-
302 12-00121.1 (2013).
- 303 27 Collins, W. D. *et al.* The integrated Earth System Model version 1: formulation and functionality.
304 *Geosci. Model Dev.* **8**, 2203-2219, doi:10.5194/gmd-8-2203-2015 (2015).
- 305 28 Bond-Lamberty, B. *et al.* On linking an Earth system model to the equilibrium carbon
306 representation of an economically optimizing land use model. *Geosci. Model Dev.* **7**, 2545-2555,
307 doi:10.5194/gmd-7-2545-2014 (2014).
- 308 29 Stainforth, D. A., Allen, M. R., Tredger, E. R. & Smith, L. A. Confidence, uncertainty and decision-
309 support relevance in climate predictions. *Philosophical Transactions of the Royal Society A:*
310 *Mathematical, Physical and Engineering Sciences* **365**, 2145-2161 (2007).
- 311 30 Strachan, N., Pye, S. & Kannan, R. The iterative contribution and relevance of modelling to UK
312 energy policy. *Energy Policy* **37**, 850-860, doi:<http://dx.doi.org/10.1016/j.enpol.2008.09.096>
313 (2009).

314 **Acknowledgements**

315 This material is based upon work supported by the U.S. Department of Energy, Office of
316 Science, Office of Biological and Environmental Research. This research used resources of the
317 Oak Ridge Leadership Computing Facility, which is a U.S. Department of Energy Office of
318 Science User Facility supported under Contract DE-AC05-00OR22725. This research used
319 resources of the National Energy Research Scientific Computing Center, a DOE Office of
320 Science User Facility supported by the Office of Science of the U.S. Department of Energy
321 under Contract No. DE-AC02-05CH11231. This work used the Community Earth System
322 Model, CESM and the Global Change Assessment Model, GCAM. The National Science
323 Foundation and the Office of Science of the U.S. Department of Energy support the CESM
324 project. The authors acknowledge long-term support for GCAM development from the
325 Integrated Assessment Research Program in the Office of Science of the U.S. Department of
326 Energy. Lawrence Berkeley National Laboratory is supported by the U.S. Department of Energy
327 under Contract No. DE-AC02 0 5CH11231. Initial research by P.E.T., J.M., and X.S. was
328 sponsored by the Laboratory Directed Research and Development Program of Oak Ridge
329 National Laboratory, managed by UT-Battelle, LLC, for the U.S. Department of Energy. We
330 thank Jay Gulledge for comments on the manuscript.

331 **Author Contributions**

332 W.D.C., J.E., A.T., B.B-L., A.D.J., and P.E.T. conceived the study. All authors contributed to
333 development of algorithms. J.T. and A.C. led the software engineering development, X.S.
334 configured and executed simulations, and M.L.B., J.M., K.C., L.C., B.B-L., and A.V.D.

335 performed diagnostics. All authors contributed to analysis of results. P.E.T., B.B.-L., A.D.J.,
336 A.V.D., K.C., L.C., X.S., and W.D.C. wrote the text, with comments and edits from all authors.

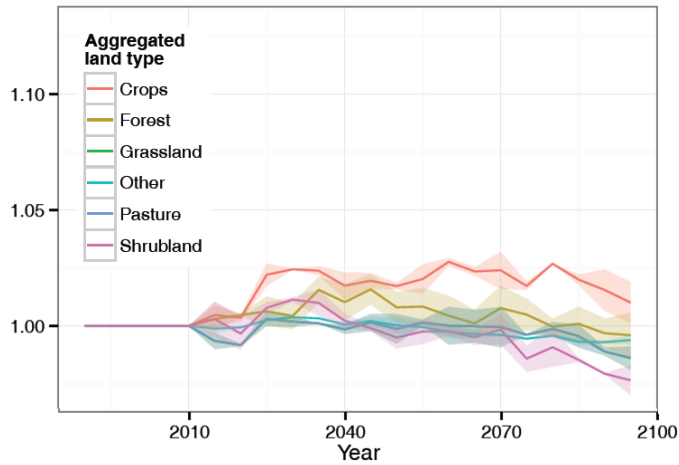
337 **Author Information**

338 The authors declare no competing financial interests. Correspondence and requests for materials
339 should be addressed to Peter E. Thornton (thorntonpe@ornl.gov).

340 **Supplemental Information**

341 Supplemental Information consists of six figures and their captions.

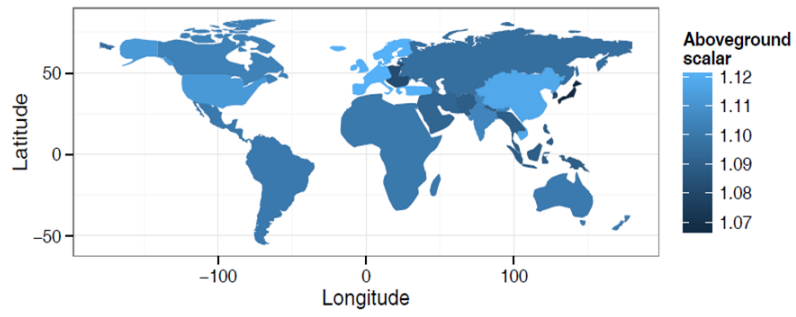
342



343

344 **Supplemental Figure 1.** Soil component of the integrated biospheric change signal passed from
345 ESM to IAM, based on changes in belowground net primary production and heterotrophic
346 respiration in the ESM relative to conditions in 1990. Signal communicated to IAM is specific to
347 each agro-ecological zone and vegetation type within zone, with plot showing area-weighted
348 global mean signal. For each aggregated land type the solid colored line shows the mean of two
349 ensemble simulations, while the shaded region of matching color shows the range of values from
350 the two ensemble members.

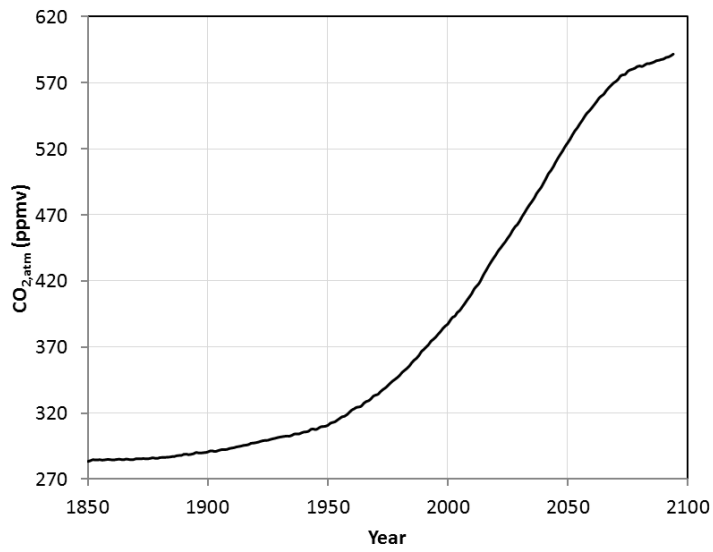
351



352

353 **Supplemental Figure 2.** Regional means for the aboveground component of integrated
354 biospheric change signal in simulation year 2094.

355

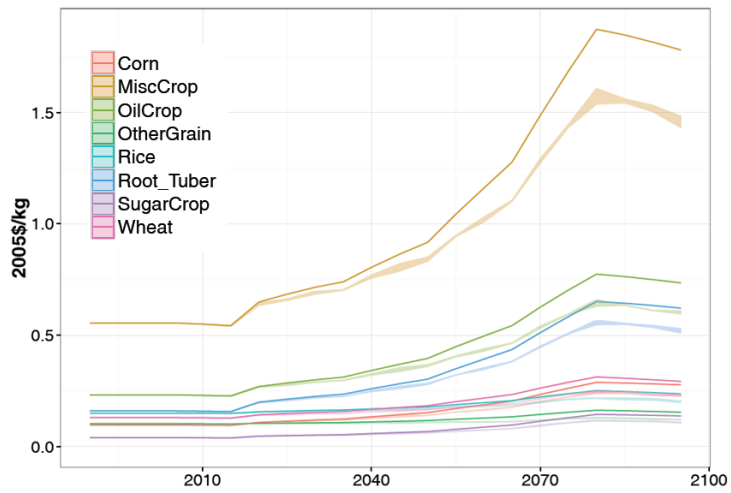


356

357 **Supplemental Figure 3.** Global mean near-surface atmospheric CO₂ from the historical transient

358 simulation (1850-2004) and a two-way synchronous coupling experiment (2005-2094).

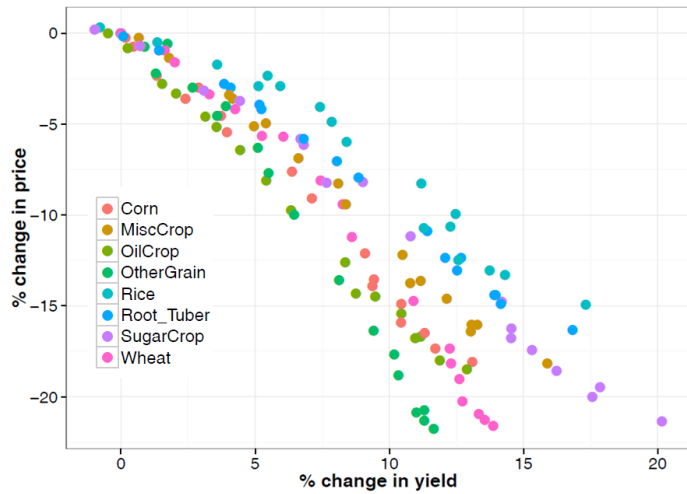
359



360

361 **Supplemental Figure 4.** Crop prices (in 2005\$/kg) for two-way coupled (shaded regions) and
 362 one-way coupled (solid lines) simulations for several major crop types. For each crop type the
 363 shaded region shows the range of values from the two ensemble members.

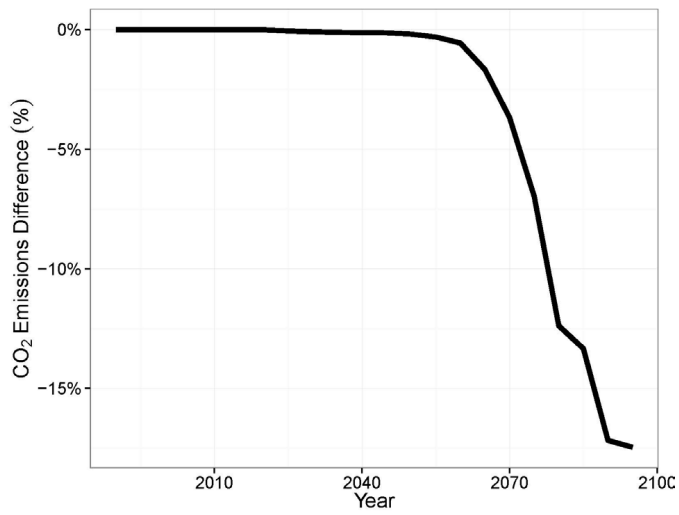
364



365

366 **Supplemental Figure 5.** Change in price for major crop types shown as a function of change in
367 yield for each crop type. Each point represents a single five-year time period (2005-2094) from
368 one ensemble simulation for a single crop, with changes shown as percent difference between
369 two-way synchronous coupled and one-way asynchronous coupled simulations. The plot
370 includes points from both ensemble simulations.

371

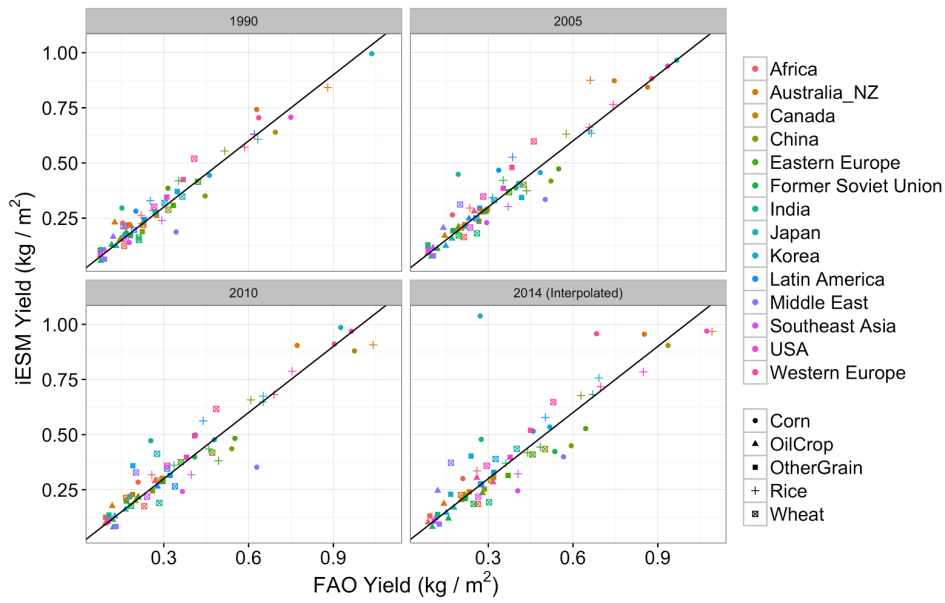


372

373 **Supplemental Figure 6.** Difference in fossil fuel CO₂ emissions as a result of biospheric change
374 feedback, shown as a percentage change between the two-way synchronous coupling and one-
375 way asynchronous coupling simulations.

376

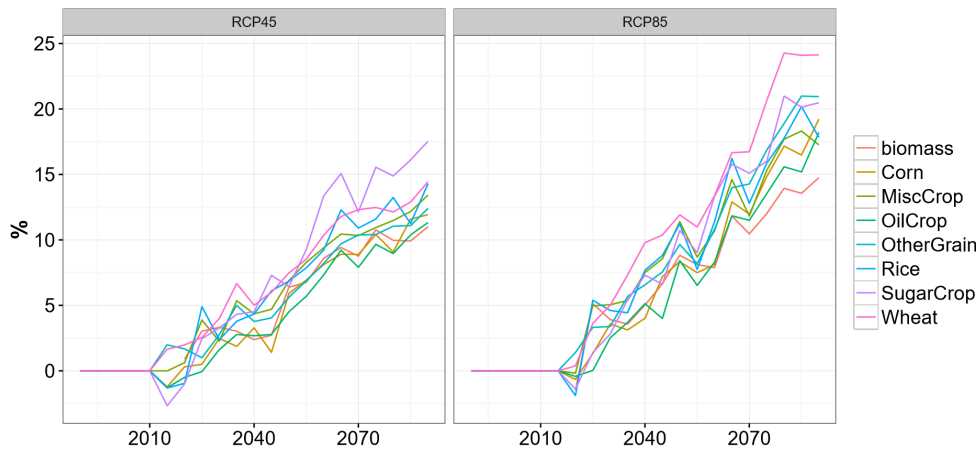
377



378

379 **Supplemental Figure 7.** Model-predicted vs. observed yield for five crops over multiple
 380 regions, for two calibration years (1990 and 2005), and two additional years (2010 and 2014).
 381 Model results for 2014 are interpolated from the actual model outputs in 2010 and 2015, to allow
 382 comparison with the most recent year for which FAO crop yield observations are available.

383



384

385 **Supplemental Figure 8.** Percent change in global mean yield for multiple crop types in the
 386 synchronous two-way coupling experiment compared to the asynchronous one-way coupling
 387 experiment, showing results for RCP 4.5 (left) and RCP 8.5 (right). Although RCP 8.5 has
 388 significantly higher CO_{2,atm} at the end of century than RCP 4.5, crop yields are only modestly
 389 higher due to the offsetting influence of more extreme radiatively-forced climate changes under
 390 RCP 8.5.

391 **Online-Only Methods**

392 **Technical description of the two-way coupled system**

393 A complete technical description for our two-way coupling framework (iESM) is published²⁷,
394 including the model formulation, requirements, implementation, testing, and functionality. The
395 complete code and analysis scripts used to generate results for this study are available from the
396 Model Archive at the ORNL DAAC [DOI to be provided prior to publication].

397 **Experimental design**

398 Our simulation experiments are initiated with radiative forcing conditions estimated circa 1850
399 AD. The 1850 initial conditions for the ESM component (land, atmosphere, ocean, and sea ice
400 state variables) are drawn from a long preindustrial control simulation (PC), in which the carbon
401 cycle on land and in the atmosphere and oceans is fully prognostic. This PC simulation is over
402 1000 years long, with predicted atmospheric CO₂ concentration varying between 281 and 287
403 ppm. Experimental simulations used in this study were performed for two time segments: a
404 historical transient (HT) segment covering the period 1850-2004, and a future scenario (FS)
405 segment covering the period 2005 to 2094.

406 During HT segments only the ESM (in our case the Community Earth System Model, CESM) is
407 active. Model inputs during HT segments, including fossil fuel emissions and land use and land
408 cover change (LULCC)⁵ are identical to those used for historical simulations in the Climate
409 Model Intercomparison Project (CMIP5).

410 Both ESM and IAM components are active for FS segments. We performed two types of
411 simulation in FS segments, differing only in the coupling method between ESM and IAM. One

412 method used asynchronous 1-way coupling (A1), in which the IAM is run in stand-alone mode
413 for the entire segment, followed by a stand-alone run of the ESM that receives LULCC and
414 emissions information saved from the IAM simulation. This is the traditional coupling approach
415 used for all CMIP5 future scenario simulations, and represented by the black arrows in Figure 1
416 (main text). The second method used synchronous 2-way coupling (S2) between the IAM and
417 ESM, corresponding to the black and red arrows in Figure 1 (main text). The S2 coupling
418 method is implemented exactly as described in the iESM technical description²⁷, except that our
419 study used a 5-year coupling time step between IAM and ESM instead of the 15-year timestep
420 described previously.

421 To ensure that the S2 coupling influence is restricted only to the passing of climate change
422 information into the crop yield and carbon stock calculations of the IAM, we use identical
423 anthropogenic fossil fuel and industrial emissions and other externally imposed radiative forcing
424 agents as input to all FS segments. The inputs used were those generated by the GCAM model
425 for the Reference Concentration Pathway (RCP) 4.5 as used in CMIP5⁶. To further constrain the
426 two-way coupled experiment, we used the GCAM carbon price pathway generated in stand-
427 alone mode (A1 type coupling) as a specified carbon price pathway for all FS segments. This
428 allows us to interpret any differences between S2 and A1 coupling methods as arising from the
429 direct influence of climate change on crop yields and carbon stocks in GCAM and the
430 subsequent influence of those changes on land-use and land-cover change predictions, without
431 needing to consider potential interactions with changing carbon price paths.

432 Our general approach to quantifying the influence of S2 vs. A1 coupling is to examine the
433 difference between two FS simulation segments, one generated using the A1 approach (FS_A1)

434 and another generated using the S2 approach (FS_S2). We refer to the difference between two
435 such FS segments as our experimental result ($ER = FS_S2 - FS_A1$).

436 Each ER includes spatio-temporal variation generated by the difference in coupling methods and
437 additional spatio-temporal variation generated by different realizations of the internal variability
438 in the ESM. By generating multiple ensemble members of ER, we can evaluate the relative
439 contributions of forced variation (the signal of interest in our analysis) and internal variation.

440 For this study we generated two ER ensemble members by initiating two separate HT segments
441 from different time points, ten years apart, in the PC simulation (HTa and HTb). We then
442 generated two FS segments starting from the endpoint of HTa, one using A1 coupling (FSa_A1)
443 and the other using S2 coupling (FSa_S2). We generated a third FS segment from the endpoint
444 of HTb, using S2 coupling (FSb_S2). The two ER ensemble members were then generated as
445 $ER1 = FSa_S2 - FSa_A1$, and $ER2 = FSb_S2 - FSa_A1$.

446 Crop yields and bioenergy production in our coupled system are calculated in the IAM
447 component. Crop yields in GCAM are calibrated against global crop data for years 1990 and
448 2005^{31, 32}. As the S2 segments progress these yields are modified by climate change information
449 passed back from the ESM. Evaluation of predicted yield by region and crop for years outside
450 the calibration period shows reasonable model performance for present-day conditions
451 [Supplemental Figure 7].

452 The influences of spatially and temporally evolving climate change factors on crop yields and
453 bioenergy production are estimated within the ESM component of our coupled system and
454 passed as scalars (multipliers) applied to yields in the IAM component. This coupling
455 arrangement is outlined in Figure 1 (main text) and described in detail in the iESM technical

456 documentation²⁷. The ESM serves as an integrator of multiple climate change factors, but it is
457 also of interest to isolate and assess contributions from individual factors. Given the uncertain
458 magnitude of CO₂ fertilization effects on crop yields¹⁸, it is of special interest to examine this
459 factor in isolation and compare to experimental estimates as possible.

460 Our study concludes that synchronous two-way coupling generates significant changes in crop
461 yields which propagate to influence crop prices, land use patterns, energy production, and fossil
462 fuel emissions. Since these diagnosed changes are due to overall increases in crop yield and
463 bioenergy production, it is possible that an overestimation of the CO₂ fertilization effect in crops
464 by the ESM could lead to an overstatement of the significance of two-way coupling effects. As
465 pointed out in the main text, our ESM component is one of a small number of such models that
466 includes the limiting influence of mineral nutrient availability on land ecosystem processes.

467 Coupling between the model representations of carbon and nutrient (nitrogen) cycles is directly
468 responsible for a significant reduction in the CO₂ fertilization effect predicted at a given CO₂
469 concentration when compared to the same model with nutrient limitation switched off³³, and
470 when compared to other models that lack nutrient limitation¹⁰. We can assert on this basis that of
471 all the existing ESMs that might be evaluated in a two-way coupling context, CESM is among
472 the two or three least likely to generate this type of overstatement of coupling effects due to high
473 bias in CO₂ fertilization.

474 Even though CESM has a CO₂ fertilization effect 2.5 times smaller than the mean of the non-
475 nutrient limited models¹⁰, it is still possible that it overestimates the influence of CO₂ fertilization
476 on crop yield compared to free-air concentration enrichment (FACE) experiments as summarized
477 for example by Long et al.¹⁸ To help further quantify this analysis, we refer to previously
478 published results from a series of single factor experiments²⁸ which included the influence of

479 historical changes in CO₂ concentration as one of the isolated factors. These results are based on
480 simulations with CESM in which the land component is forced with a multi-year repeating cycle
481 of surface weather data, while other factors such as CO₂ concentration, nitrogen deposition, or
482 land use are allowed to vary (one at a time) according to their observed historical trajectories
483 over the years 1850-2010.

484 In those simulations a gradual rise in CO₂ concentration of 110 ppmv (from 280 ppmv in year
485 1850 to 390 ppmv in year 2010) produced a ~7% increase in gross primary production
486 (photosynthesis) and in net primary production (NPP, or vegetation growth). That simulation
487 result is not directly comparable to the FACE experimental regime, since the model result is
488 based on a gradual increase in CO₂ while the FACE experiments involve a step-change. Also, the
489 FACE experiments started from modern CO₂ concentrations and increased concentration by
490 about 200 ppmv, arriving at values around 550 ppmv. Chamber studies suggest that crop yield
491 responses to CO₂ concentrations between 380 and 600 ppmv are approximately linear, and our
492 offline model results are linear over the range 280 to 390 ppmv. It is reasonable to estimate,
493 based on simple linear scaling, that the ~7% increase in NPP for the increase in atmospheric CO₂
494 from 280 to 390 ppmv would correspond to an increase in NPP of 12% for an increase in CO₂
495 similar to the FACE experiments. We are not able to quantify the potential influence of gradual
496 vs. step change in CO₂ concentration from the available results.

497 Since NPP from CESM is passed to the IAM in our synchronously coupled system as a scalar
498 (multiplier) on crop yields, a useful comparison with FACE results is from a synthesis for CO₂
499 enrichment effects on crop yields¹⁸, which summarized the FACE results for rice, wheat and
500 soybean yields as 12%, 13%, and 14% increase, respectively. The major difference between our
501 model results and the FACE crop synthesis¹⁸ is for C₄ crops. CESM includes a C₄ grass type, and

502 although the underlying physiology model does not predict a significant response to CO₂
503 fertilization in this type through an influence on leaf-scale photosynthetic rate, effects of CO₂
504 concentration on stomatal conductance are included for C₄ types, and NPP increases for C₄ types
505 in the single-factor experiment are similar to increases for C₃ types due to indirect effects on soil
506 water status. This is in contrast to the FACE synthesis, which found no effect of enriched CO₂
507 concentration on C₄ crop yield (based on one year of data from one study).

508 In follow-on work, we are improving the representation of multiple crop types directly within the
509 ESM component, so that information can be passed with less aggregation between the ESM and
510 IAM components in future coupling simulations.

511 We include a single pair of simulation experiments for the RCP 8.5 scenario, as a preliminary
512 test of the generality of our RCP 4.5 results. The RCP 8.5 simulations start from the same HT
513 endpoint as described above for RCP 4.5, and follow a common simulation protocol. Only one
514 A1 and one S2 simulation was performed for RCP 8.5, so the results described in the main text
515 and illustrated in Supplemental Figure 8 reflect only a single ensemble member.

516 **Additional References for Online-Only Methods**

517 ³¹ FAOSTAT. Food and Agriculture Organization of the United Nations. Rome, Italy.
518 (faostat3.fao.org) (2014)

519 ³² Kyle, P., P. Luckow, K. Calvin, W. Emanuel, M. Nathan and Y. Zhou. GCAM 3.0
520 Agriculture and Land Use: Data Sources and Methods. Richland, WA, Pacific Northwest
521 National Laboratory. (2011)

522 ³³ Thornton, P. E., J.-F. Lamarque, N. A. Rosenbloom and N. M. Mahowald. Influence of
523 carbon-nitrogen cycle coupling on land model response to CO₂ fertilization and climate
524 variability. *Global Biogeochemical Cycles* **21**(4): GB4018 doi:10.1029/2006GB002868.
525 (2007)